RSC Advances

RSC Advances

Journal Name

ARTICLE

A detailed study on the thermal, photo-physical, electrochemical properties and OFET applications of D-π-A-π-D structured unsymmetrical diketopyrrolopyrrole materials

D. Bharath,[a] S. Chithiravel,[b] M. Sasikumar,[a] Narendra Reddy Chereddy,[a,]* S. Balaih,[c] K. Bhanuprakash,[c,]* K. Krishnamoorthy[b,]* and V. Jayathirtha Rao[a,d]*

A series of seven unsymmetrical diketopyrrolopyrrole (DPP) derivatives with donor-pi-acceptor-pi-donor (D-π-A-π-D) architecture have been designed, synthesized and well characterised. Effect of the electron donating capacity and extent of electronic conjugation of the end-capping units on the thermal, photo-physical and electrochemical properties of the synthesized materials was thoroughly investigated using various experimental techniques and theoretical calculations. Organic field-effect transistors (OFETS) were fabricated using these materials to obtain their hole/electron transporting characteristics. All these materials show moderate to good hole transporting ability and the OFET fabricated using DPP-derivative with benzofuran and pyrene end groups exhibited the hole mobility of 6.7 x 10^{-4} cm^2/Vs with V_T of -9 V. The observed photo-physical, electrochemical, thermal, and charge carrier properties of the synthesized DPP-derivatives indicated their applicability in various areas like organic photovoltaics, disposable electronics and biomedical devices.

Introduction

During the last couple of decades, organic materials with donor-acceptor (D-A) architecture have been attracted a great deal of attention by the researchers owing to their promising applications in various fields like organic field-effect transistors (OFETs), organic photovoltaics (OPV) and organic light-emitting devices (OLEDs).[1] Organic materials with the combination of donor (D) and acceptor (A) moieties can show broad visible region absorption and narrow optical band gap due to the intramolecular charge transfer (ICT) character between the donor and acceptor moieties. Broad visible region absorption and narrow optical band gap are prerequisite for the materials to show efficient light harvesting property over the entire solar spectrum and high charge carrier mobility.[2] Hence numerous reports are available in the literature based on the materials with D-A architecture.[3] In the last few years extensive efforts have been made by the researchers to diversify the D-A materials and materials with various structural motifs like symmetrical D-A-D or A-D-A, or even more complex combinations such as linear A-D-A-D-A, D-A-D-A-D are

developed for optoelectronic applications.[4]

Among various building blocks, diketopyrrolopyrrole (DPP) has been extensively studied to develop materials for various applications owing to its facile synthetic procedures and excellent properties like good thermal and photo stabilities, high planarity and ambipolar charge carrier transport.[5] Many high performance DPP-based polymers are available in the literature for OPV and OFET applications.[5d] Excellent intermolecular solid state aggregation of the DPP derivatives in their polymers improve their charge carrier mobilities and leads to highly efficient organic semiconductors.[2b, 6] Small molecular semiconducting materials are advantageous over their polymer counterparts in terms their simpler synthesis

[a] Crop Protection Chemicals Division, CSIR-Indian Institute of Chemical Technology, Hyderabad-500007, India. Email: chereddynarendra@gmail.com; jrao@iict.res.in
[b] Polymers and Advanced Materials Laboratory, CSIR-National Chemical Laboratory, Pune-411008, India. Email: k.krishnamoorthy@ncl.res.in
[c] Inorganic and Physical Chemistry Division, CSIR-Indian Institute of Chemical Technology, Hyderabad-500007, India
[d] AcSIR, CSIR-Indian Institute of Chemical Technology, Hyderabad-500007, India
† Footnotes relating to the title and/or authors should appear here.
Electronic Supplementary Information (ESI) available: [NMR, ESI-HRMS, DSC, solvent dependent changes, theoretical calculations and charge transport properties are provided]. See DOI: 10.1039/x0xx00000x
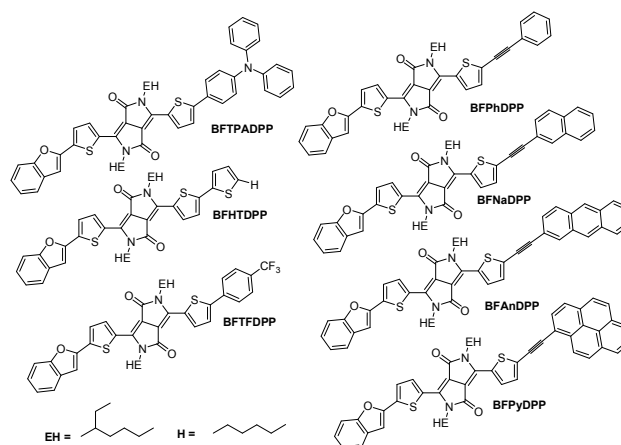

Fig. 1. Chemical structures of the synthesized DPP-derivatives.

and purification procedures, lower batch-to-batch variation, and greater reproducibility.[7] After the pioneering work of Nguyen *et al* on DPP functionalized oligothiophene for solution-processed BHJ solar cells, several small molecular DPP derivatives are reported with a variety of applications.[8]

Modulation of the molecular backbone with variations in their donor aromatic groups as end-capping units has a great impact not only for improving the molecular optoelectronic properties but also to control aggregation of the materials.[4b, 9] Even though several DPP based small molecular semiconducting materials with symmetrical D-A-D architecture are reported, studies on the unsymmetrical DPP materials are very rare. Keeping this in mind, in the present work we have synthesized a series of unsymmetrical DPP derivatives with different end capping units by anticipating that selection of appropriate end capping units can impart better properties compared to their symmetrical analogues. The synthesized unsymmetrical DPP materials have benzofuran at one end and chemical entities with different electron donating capacity and various extents of electronic conjugation are at the second side. Optoelectronic properties of the synthesized DPP-derivatives are studied using UV-visible, fluorescence, time-resolved fluorescence spectroscopic techniques and cyclic voltammetric analysis. OFETs are fabricated using the synthesized DPP derivatives to understand the effect of the end-capping units on their charge carrier mobilities. The observed properties of the synthesized unsymmetrical DPP derivatives are compared with their symmetrical analogue dibezofuran-DPP **DPP(TBFu)$_2$**.

Results and discussion

Molecular structures and thermal properties

Molecular structures of the synthesized DPP-derivatives are shown in **Fig. 1**. All the DPP-derivatives reported here contain benzofuran as one end-capping unit and they differ structurally only in use of other end-capping groups. The DPP-derivatives, **BFTPADPP**, **BFHTDPP** and **BFTFDPP** contain electron donating triphenylamine (TPA), 2-hexylthiophene (HT) and electron withdrawing p-trifluoromethylphenyl (TF) moieties, respectively as end-capping units and the derivatives **BFPhDPP**, **BFNaDPP**, **BFAnDPP** and **BFPyDPP** possess phenyl (Ph), naphthyl (Na), anthracenyl (An) and pyrenyl (Py) end groups that have various extents of electronic conjugation,
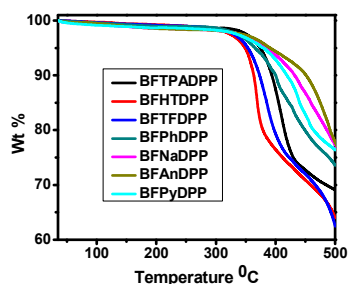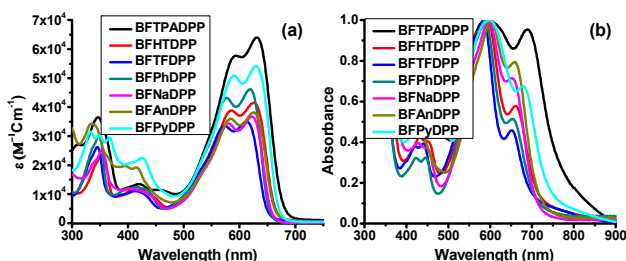
Table 1. Thermal data of the synthesized DPP-derivatives

Material Code	Decomposition temperature (T_d) ^{0}C	Melting temperature (T_m) ^{0}C	Glass transition temperature (T_g) ^{0}C	Crystallization temperature (T_c) ^{0}C
BFTPADPP	373.5	190.3	74.7	124.3
BFHTDPP	348.7	140.1	-	103.1
BFTFDPP	352.4	207.0	-	-
BFPhDPP	364.8	121.7	-	-
BFNaDPP	387.2	185.3	-	-
BFAnDPP	390.9	-	-	-
BFPyDPP	379.7	193.7	79.2	130.9

respectively. A triple bond is introduced for the derivatives **BFPhDPP**, **BFNaDPP**, **BFAnDPP** and **BFPyDPP** by assuming that insertion of a triple bond can provide sufficient space to minimize the steric hindrance between the neighboring moieties and helpful to improve the planarity of the materials. These structural manipulations among the seven compounds certainly help for an effective investigation on the effects of end-capping substitutions on their optoelectronic properties. Synthetic scheme, detailed synthetic procedure of the reported DPP-derivatives are provided in ESI† and thesynthesized materials were thoroughly characterized using NMR (Figs. S1-S14, ESI†) and ESI-HRMS (Figs. S15-S21, ESI†) analyses. The synthesized DPP-derivatives had good solubility in common organic solvents such as CHCl$_3$, THF, O-dichlorobenzene and toluene, which is essential for solution processability in device fabrication.

High thermal stability is an important requirement for the materials for practical applications. Therefore, thermal properties of the synthesized DPP-derivatives were investigated using thermogravimetric analysis (TGA) and differential scanning colorimetry (DSC). TGA curves and the corresponding data of these materials are provided in **Fig. 2** and Table 1, respectively. All the synthesized materials showed the decomposition temperatures (T_d, defined as that at which 5 wt % loss is observed) above ~348 ^{0}C, indicating their high thermal stability and suitability for vacuum deposition techniques. DSC thermograms of these DPP-derivatives are provided in Fig. S22, ESI†. All the derivatives except **BFAnDPP** showed sharp endotherms corresponding to their melting temperatures. Among the derivatives **BFPhDPP**, **BFNaDPP** and **BFPyDPP**, melting temperatures were gradually increased from **BFPhDPP** to **BFPyDPP** and **BFPyDPP** showed highest melting temperature (193.7 ^{0}C) while **BFPhDPP** displayed the lowest (121.7 ^{0}C). This observed gradual increment in the melting temperatures might be due to increase in their molecular weights as well as improvement in their molecular planarity that results in better intermolecular stacking.[10] Among the derivatives **BFTPADPP**, **BFHTDPP** and **BFTFDPP**, **BFTFDPP** exhibited highest melting temperature (207.0 ^{0}C) followed by **BFTPADPP** (190.3 ^{0}C) and **BFHTDPP** (140.1 ^{0}C). Apart from their melting endotherms, derivatives **BFTPADPP**, **BFPyDPP** and **BFHTDPP** displayed exothermic peaks at 124.3, 130.9 and 103.1 ^{0}C, respectively corresponding to their crystallization temperatures upon first heating and first cooling cycles. The melting (T_m), glass transition (T_g) and crystallization

Fig. 2. TGA thermograms of the synthesized DPP-derivatives

Fig. 3. UV-visible absorption spectra of the synthesized DPP-derivatives (10 μM) in chloroform solution (**a**) and their normalized absorption spectra in thin film state (**b**)

temperatures (T_c) of the synthesized DPP-derivatives are provided in Table 1.
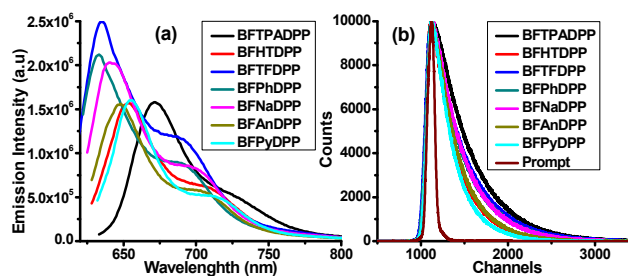
Photo-physical characteristics

The UV-visible absorption characteristics of the reported DPP-derivatives were measured in both solution and thin film states. **Fig. 3a** shows the UV-visible absorption spectra of these materials in chloroform solution and the corresponding data is provided in Table 2. All the DPP-derivatives showed two primary absorption bands in the visible region ranging 370–480 nm and 490–700 nm that are quite different from their mono-bromo synthetic precursor (Fig. S23, ESI†) and indicated efficient electronic coupling between the DPP core and the end-capping moieties. The absorption bands in the shorter wavelength region are attributed to the localized $\pi - \pi*$ transitions and the absorption bands at longer wavelength region are ascribed to the charge transfer (CT) between the end-capping units and DPP central core.[8] Among the DPP-derivatives reported here, **BFTPADPP** with electron donating TPA end group exhibited the highest absorption maxima (λ_{max}, ~630.6 nm) and **BFTFDPP** with electron withdrawing TF end group showed the lowest λ_{max} of 613.5 nm. DPP-derivatives **BFPhDPP**, **BFNaDPP**, **BFAnDPP** and **BFPyDPP** with Ph, Na, An and Py end-capping groups had similar absorption maxima ~619.0, 622.0, 625.2, and 629.4 nm, respectively. These observations clearly suggested that compared to the extent of electronic conjugation, electron donating tendency of the end-capping units had significant effect on their absorption maxima. Effect of solvent polarity on the ground state absorption of the synthesized DPP-derivatives was estimated by observing their UV-visible absorption pattern in different

solvents and the corresponding absorption spectra are provided in Fig. S24, ESI†. All the derivatives except **BFPyDPP** showed only modest variations in their absorption pattern in different solvents revealing that solvent polarity has insignificant role on their ground state absorption. The observed significant deformation in the absorption band of **BFPyDPP** might be ascribed to the improved intermolecular interactions in MeOH solution. Absorption spectra of the DPP-derivatives in their thin film state are shown in **Fig. 3b**. Compared to the solution state (**Fig. 3a**), the absorption bands of the DPP-derivatives were significantly broadened and developed new CT bands at longer wavelength region.[10,11] Interestingly, among **BFTPADPP**, **BFHTDPP** and **BFTFDPP**, the CT bands are more pronounced for **BFTPADPP** followed by **BFHTDPP** and **BFTFDPP**. This marked difference in the thin film state absorption profiles of **BFTPADPP**, **BFHTDPP** and **BFTFDPP** could be attributed to the variations in their solid-state arrangement as a result of the intermolecular donor-acceptor interactions between the DPP central core and the end-capping units.[12] Since TPA is electron-rich, it can couple strongly to the electron deficient DPP core of adjacent molecules resulting in head-to-tail type J-aggregation. As a consequence of low electron donating capacity of HT and TF compared to TPA, they could not maintain strong intermolecular donor-acceptor interactions with the DPP central core of the neighbouring molecules and hence resulted in low intensity CT bands in their thin film absorption spectra.[12] Similarly in the case of derivatives **BFPhDPP**, **BFNaDPP**, **BFAnDPP** and **BFPyDPP**, the intensity of longer wavelength CT bands was increased with the extent of electronic conjugation of the end groups, which might be due to the improved the donor-acceptor (D-A) interactions in the materials with the end-capping units having high electronic conjugation.[10] It is imperative to note that in thin film state, all the synthesized DPP-derivatives have enhanced visible region light harvesting ability compared to their symmetrical DPP-analogues[10,13] and it could be attributed to the improved planarity and efficient ICT between the end-capping units and DPP central core of these materials. Optical band gaps of the synthesized DPP-derivatives were estimated from the onsets of their thin film absorption spectra and the values are provided in Table 2.

Fig. 4a depicts the emission spectra of the synthesized DPP derivatives in chloroform solution. All the synthesized

Table 2. Photo-physical data of the synthesized DPP-derivatives

Material Code	$\lambda_{max\ Abs}$ (nm) (ε, $M^{-1}\ Cm^{-1}$)	$\lambda_{max\ Emi}$ (nm)	Emission lifetime (τ, ns)	λ_{onset} film (nm)	Band gap (E_{opt})
BFTPADPP	630.6 (64454)	671.4	2.82	789.7	1.57
BFHTDPP	627.3 (41885)	653.6	1.95	760.1	1.63
BFTFDPP	613.5 (35230)	635.2	2.68	729.3	1.70
BFPhDPP	619.0 (46667)	632.7	2.46	734.3	1.69
BFNaDPP	622.0 (37066)	641.4	2.40	742.2	1.67
BFAnDPP	625.2 (38443)	648.1	1.97	754.2	1.64
BFPyDPP	629.4 (54432)	655.5	1.66	771.9	1.61

Fig. 4. Emission spectra (**a**) and lifetime decays (**b**) of the synthesized DPP-derivatives in chloroform solution

derivatives showed two well-resolved bands in their emission spectra that are characteristic to DPP.[14] Among all the derivatives synthesized, **BFTPADPP** showed the highest (671.4 nm) and **BFPhDPP** and **BFTFDPP** (632.7 and 635.2 nm, respectively) showed the lowest emission maxima in accordance with their absorption pattern indicating that TPA end group imparted improved charge delocalization compared to the other end groups used in this study. Emission spectra of these derivatives in different solvents were recorded and the spectra are provided in Fig. S25, ESI†. The observed solvent dependent variations in the emission maxima of the synthesized DPP-derivatives were much pronounced compared to their solvent dependant changes in the absorption maxima (Fig. S24, ESI†). These results indicated that solvent-solute interactions are higher in their excited state compared to the ground state.

In sharp contrast, the synthesized donor materials in their thin film state displayed a broad and structure less emission in the region of 700–810 nm (Fig. S26, ESI†). Moreover, the fluorescence emission intensity of these materials in their thin film state was drastically reduced relative to their fluorescence emission in solution state (**Fig. 4a**). These observed differences in the fluorescence dynamics of the synthesized DPP-derivatives in thin film and solution states clearly indicated the possibility for intermolecular electron transfer among the DPP-derivatives in their thin film state that facilitates non-radiative deactivation of the excited state materials.[15] The fluorescence lifetimes of these DPP-derivatives were estimated in their solution state using time correlated single photon counting (TCSPC) technique (**Fig. 4b**) to understand the lifetime of the excitons formed upon absorption of light. All the derivatives showed nearly equal excited singlet state lifetime profiles and the observed fluorescence lifetimes are provided in Table 2. The emission decay profiles with their corresponding fit curves are shown in Fig. S27, ESI†.

To understand the origin of the spectroscopic properties of the DPP-derivatives observed in solution, density functional theory (DFT) and time-dependent density functional theory (TD-DFT) calculations were performed on these molecules using Gaussian 09 with the functionals B3LYP (Table S1-S2, ESI†), M06-2X (Table S3, ESI†) and cam-B3LYP (Table S4, ESI†) combined with 6-31G (d, p) basis set. The alkyl groups of the DPP-derivatives were replaced with methyl groups to simplify the calculations. Optimized structures of the DPP-derivatives and their corresponding highest occupied molecular orbital (HOMO) and the lowest unoccupied molecular orbital (LUMO) wave functions are illustrated in **Fig. 5**. Both the HOMO and LUMO wave functions are delocalized over the DPP, thiophene and end-capping fragments. All the DPP-derivatives except **BFTPADPP** (bulky TPA end-capping unit) have planar molecular geometry . No considerable intramolecular twist was observed by changing the end-capping units (**Fig. 5**). All the DPP-derivatives show low ground state dipole moments (Table S1, ESI†) and these low ground state dipole moments could be the reason for the observed mild sensitivity of their absorption profiles towards the solvents with various polarities. TD-DFT calculations were also conducted and the theoretically derived
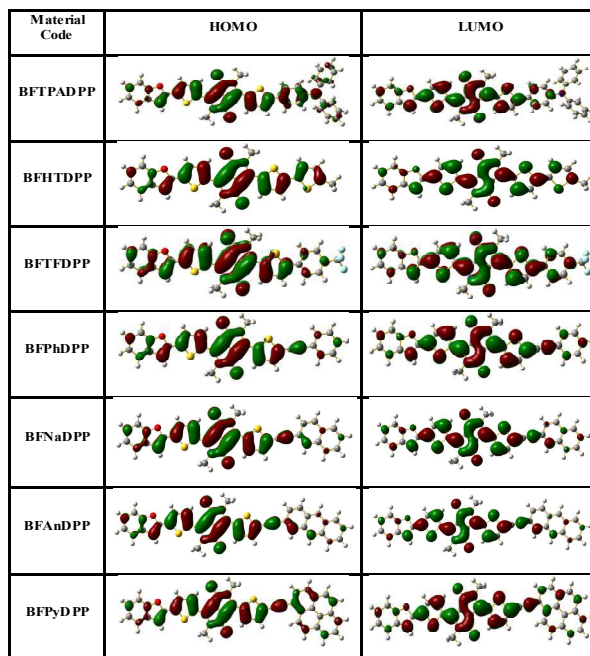

Material Code	HOMO	LUMO
BFTPADPP		
BFHTDPP		
BFTFDPP		
BFPhDPP		
BFNaDPP		
BFAnDPP		
BFPyDPP		

Fig. 5. HOMO and LUMO distributions of the synthesized DPP-derivatives

absorption spectra obtained in chloroform solvent phase using the B3LYP/6-31G (d,p) method (Fig. S28, ESI†) are in good agreement with the experimental results (**Fig. 3a**).[16] Whereas the λ_{max} of these derivatives obtained using M06-2X/6-31G (d,p) and cam-B3LYP/6-31G (d,p) in chloroform solvent are slightly under estimated though the trend is reproduced. According to results of the TD-DFT calculations, the observed long wavelength absorption band (630-700 nm) of the DPP-derivatives correspond to the $S_0{\rightarrow}S_1$ transitions and is dominated by HOMO→LUMO transition (Table S2, ESI†). The results of TD-DFT calculations also indicate that these molecules have high ground to excited state transition dipole moments. The HOMO, LUMO energy levels, adiabatic ionization potential (IP_A) and electron affinity (EA_A) values of the synthesized DPP-derivatives estimated from the theoretical calculations and the values experimentally obtained are in good agreement.

Electrochemical characteristics

Electrochemical properties of the DPP based materials reported here were investigated using cyclic voltammetry (CV). All the CV experiments were performed at room temperature with a conventional three electrode setup consisting of a glassy carbon working electrode, standard calomel electrode (SCE) and platinum wire as reference and counter electrodes, respectively. The potential of reference electrode was calibrated using ferrocene internal standard. All the measurements were conducted in anhydrous dichloromethane media, under nitrogen atmosphere using Bu_4NClO_4 (0.1 M) as supporting electrolyte at a scan rate of 100 mV/S. All the
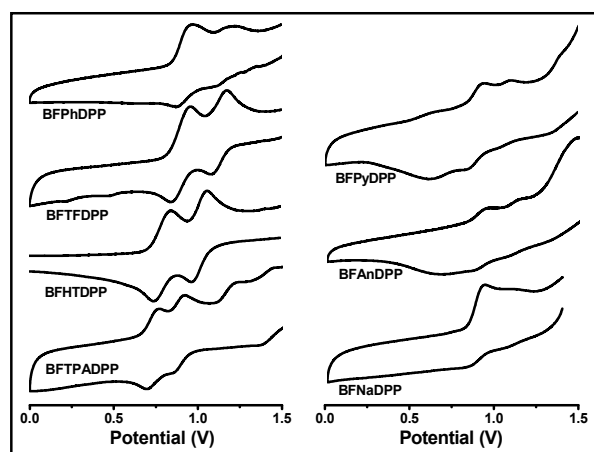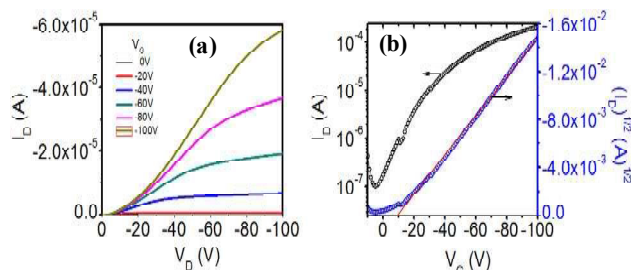
Fig. 6. Cylcic voltagramms represent the reversible oxidation behaviour of the synthesized DPP-derivatives

Fig. 7. Typical output curve (**a**) and transfer curve (**b**) of **BFPyDPP**

derivatives displayed reversible (and quasi reversible) oxidation and reduction behaviour (**Fig. 6** and Fig. S29, ESI†) and the respective onset oxidation and reduction potentials are provided in Table 3. The oxidation potentials of the DPP-derivatives were sensitive to the nature of the end groups. Among all the DPP-derivatives, **BFTPADPP** showed lower oxidation potential (+ 0.67 V) owing to the easily oxidisable nature of the electron donating TPA end-capping unit and the oxidation potentials of the DPP-derivatives increased with decreasing the electron donating tendency of the end groups (0.72 and 0.81 V respectively for **BFHTDPP** and **BFTFDPP**). On the other hand, the extent of electronic conjugation of the end groups had negligible effect on their oxidation potentials.[10] The DPP-Derivatives **BFPhDPP**, **BFNaDPP**, **BFAnDPP** and **BFPyDPP** had similar oxidation potentials 0.85, 0.84, 0.83 and 0.82, respectively. The corresponding HOMO energy levels of these derivatives were estimated from their oxidation potentials using the ferrocene reference value of -4.4 eV below the vacuum level[17] and the values are provided in Table 3. The LUMO values of the synthesized DPP-derivatives were calculated from their onset reduction potentials obtained from cyclic voltammetry and the values are included in Table 3. The calculated HOMO and LUMO energy levels of these DPP-derivatives (5.07-5.25 and 3.41-3.49 eV, respectively) were well matched with the work functions of commonly used gold and silver cathodes (5.1 and 4.7 eV, respectively) indicating the possibility for efficient charge injection and improved charge carrier mobility.[18] It is interesting that even though all the

synthesized DPP-derivatives have extended visible region light harvesting ability, their HOMO energy levels was considerably low laid (except for **BFTPADPP** and **BFHTDPP**) compared to the well studied symmetrical dibenzofuran-DPP, **DPP(TBFu)$_2$** (-5.14 eV).[13a] This low laid HOMO energy levels can certainly help to improve the open circuit voltage (V_{oc}) of the BHJ devices fabricated using these materials. Hence the results of the UV-visible and CV experiments suggested that by selecting appropriate end-capping units, unsymmetrical DPP-derivatives can show better properties over their symmetrical analogues.

Charge carrier mobility measurements

The charge transport properties of the synthesized DPP-derivatives were measured in organic field-effect transistors (OFETs). The device configuration was bottom gate bottom contact with gold electrodes as source and drain contacts. The gate dielectric was 230 nm thick SiO$_2$. The gate electrode was heavily doped silicon. All the materials were spun on the substrate from chloroform solution. The output characteristics was measured by sweeping the drain voltage between 0 and -100 V and holding the gate voltage at various constant potentials (**Fig. 7a**). All the synthesized DPP-derivatives exhibited hole transporting ability in this configuration and displayed clear linear and saturation regimes (Fig. S30-S33, ESI†). It should be noted that the linear regime didn't start at 0 V, indicating the possibility of contact resistance and charge traps.[19] The charge carrier mobility was calculated using linear and saturation regimes.[20] The OFET parameters for these DPP-derivatives are summarized in Table 4. All the synthesized DPP-derivatives showed moderate to good hole transporting ability and among all these derivatives, highest hole mobility was measured for **BFPyDPP** (6.7×10^{-4} cm^2/Vs) with V_T of -9 V (**Fig.**

Table 3. Electrochemical data of the synthesized DPP-derivatives

Material Code	$E_{+1/2}{}^{+/0}$ (V)	HOMO (eV)[a]	$E_{1/2}{}^{0/-}$ (V)	LUMO (ev)[b]	Band gap[c] ($E_{e\ chem}$)
BFTPADPP	0.67	-5.07	-0.99	-3.41	1.66
BFHTDPP	0.72	-5.12	-0.96	-3.44	1.68
BFTFDPP	0.81	-5.21	-0.94	-3.46	1.75
BFPhDPP	0.85	-5.25	-0.98	-3.42	1.83
BFNaDPP	0.84	-5.24	-0.94	-3.46	1.78
BFAnDPP	0.83	-5.23	-0.93	-3.47	1.76
BFPyDPP	0.82	-5.22	-0.91	-3.49	1.73

Table 4. Field-effect transistor data of the synthesized DPP-derivatives

7b). The highest mobility in **BFPyDPP** is likely due to the better

Material code	Mobility(cm^2/Vs) saturation regime	Mobility(cm^2/Vs) Linear regime	V_T (V)	$I_{on/off}$
BFTPADPP	8.85×10^{-5}	4.95×10^{-5}	-5	2.02×10^2
BFHTDPP	1.12×10^{-4}	1.02×10^{-4}	-20	9.17×10^2
BFTFDPP	2.25×10^{-5}	1.35×10^{-5}	-38	3.01×10^2
BFPhDPP	2.16×10^{-4}	2.02×10^{-4}	-18	1.12×10^2
BFNaDPP	2.70×10^{-5}	4.22×10^{-5}	-11	7.92×10^1
BFAnDPP	4.72×10^{-6}	3.37×10^{-6}	-10	8.30×10^2
BFPyDPP	6.74×10^{-4}	4.11×10^{-4}	-9	7.02×10^1

packing between the molecules due to the presence of flat pyrene as one terminal moiety. In line with the results of DSC analysis (Fig. S22, ESI†), DPP-derivatives with crystalline nature (**BFTPADPP**, **BFHTDPP** and **BFPyDPP**) displayed better hole mobilities compared to the other DPP-derivatives reported here. However, it is not appropriate to comment on the absolute solid-state packing of these materials without single-crystal structures. Among the synthesized DPP-derivatives, **BFHTDPP** (1.1×10^{-4} cm^2/Vs) and **BFPhDPP** (2.2×10^{-4} cm^2/Vs) displayed comparable hole transporting characteristics with **DPP(TBFu)$_2$** (1.6×10^{-4} cm^2/Vs), while **BFPyDPP** exhibited four times better hole transporting ability.[21] **BFTFDPP** output and transfer characteristic curves showed ambipolar charge transport (Fig. S31, ESI†) owing to the presence of electron withdrawing TF end-capping unit. The hole mobility was found to be 2.2×10^{-5} cm^2/Vs. However, it was not possible to calculate the electron mobility due to the absence of clear linear and saturation regimes.

Conclusions

Seven unsymmetrical DPP-derivatives namely **BFTPADPP**, **BFHTDPP**, **BFTFDPP**, **BFPhDPP**, **BFNaDPP**, **BFAnDPP** and **BFPyDPP** with D-π-A-π-D architecture have been synthesized and are well characterised using NMR, ESI-HRMS analytical techniques. Optoelectronic properties of the synthesized DPP derivatives are measured and the effect of end capping units on their optoelectronic properties is explored. The obtained values are compared with their symmetrical analogue dibenzofuran-DPP **DPP(TBFu)$_2$**. All the synthesized derivatives show improved UV and visible region light harvesting ability compared to **DPP(TBFu)$_2$**. Among all the DPP-derivatives studied, **BFTPADPP** with electron donating TPA end-capping unit displayed highest light absorption capacity indicating that the electron donating capacity of the end capping units has significant role on their absorption profiles. The estimated HOMO and LUMO energy levels of the synthesized materials are in agreement with the work functions of the most commonly used cathode materials (Au and Ag) and as well as with the fullerene acceptors (PC$_{60}$BM and PC$_{70}$BM). The HOMO energy levels of the synthesized DPP derivatives are considerably low laid (except for **BFTPADPP** and **BFHTDPP**) compared to **DPP(TBFu)$_2$**. OFETs are fabricated using these materials and they show moderate to good charge carrier mobilities. Among the OFETS fabricated, OFETs with **BFPyDPP** exhibited the best performance characteristics with the hole mobility of 6.7×10^{-4} cm^2/Vs with V_T of -9 V and the observed mobility is four times better compared to OFETs with **DPP(TBFu)$_2$**. Excellent thermal stability, good light harvesting capacity with appropriate energy levels and good charge carrier mobilities designated the utility of these materials in various applications like organic BHJ solar cells, disposable electronics and biomedical devices. Moreover, this study also reveals that development of unsymmetrical DPP-based materials by selecting suitable end-capping units gives us a wide scope for obtaining materials with appropriate photo-physical, electrochemical and charge transport properties.

Notes and references

1   (a) Organic Electronics: Materials, Manufacturing and Applications, ed. H. Klauk, Wiley-VCH, Weinheim, Germany, 2006; (b) C. B. Nielsen, M. Turbiez and I. McCulloch, *Adv. Mater.*, 2013, **25**, 1859; (c) J. D. Yuen and F. Wudl, *Energy Environ. Sci.*, 2013, **6**, 392; (d) S. Radhakrishnan and N. Somanathan, *J. Mater. Chem.*, 2006, **16**, 2990 (e) J-H. Jou, S. Kumar, P-H. Fang, A. Venkateswararao, K. R. J. Thomas, J-J. Shyue, Y-C. Wang, T-H. Li and H-H. Yu, *J. Mater. Chem. C*, 2015, **3**, 2182.

2   (a) S. Roquet, A. Cravino, P. Leriche, O. Aleveque, P. Frere and J. Roncali, *J. Am. Chem. Soc.*, 2006, **128**, 3459; (b) C. Kanimozhi, N. Yaacobi-Gross, K. W. Chou, A. Amassian, T. D. Anthopoulos and S. Patil, *J. Am. Chem. Soc.*, 2012, **134**, 16532; (c) Y. J. Cheng, S. H. Yang and C. S. Hsu, *Chem. Rev.*, 2009, **109**, 5868.

3   (a) Y. Shirota and H. Kageyama, *Chem. Rev.*, 2007, **107**, 953; (b) K. Müllen and G. Wegner, Electronic Materials: The Oligomer Approach, Wiley-VCH, Weinheim, Germany, 1998; (c) B. Tieke, A. R. Rabindranath, K. Zhang and Y. Zhu, Beilstein *J. Org. Chem.*, 2010, **6**, 830.

4   (a) B. Walker, C. Kim and T. Q. Nguyen, *Chem. Mater.*, 2011, **23**, 470; (b) Y. Z. Lin, Y. F. Li and X. W. Zhan, *Chem. Soc. Rev.*, 2012, **41**, 4245; (c) A. Mishra and P. Bauerle, *Angew. Chem., Int. Ed.*, 2012, **51**, 2020; (d) J. Li, K. H. Ong, S. L. Lim, G. M. Ng, H. S. Tan and Z. K. Chen, *Chem. Commun.*, 2011, **47**, 9480; (e) S. Loser, C. J. Bruns, H. Miyauchi, R. P. Ortiz, A. Facchetti, S. I. Stupp and T. J. Marks, *J. Am. Chem. Soc.*, 2011, **133**, 8142.

5   (a) H. Bronstein, Z. Chen, R. S. Ashraf, W. Zhang, J. Du, J. R. Durrant, P. S. Tuladhar, K. Song, S. E. Watkins, M. Geerts, M. M. Wienk, R. A. J. Janssen, T. Aothopoulos, H. Sirringhaus, M. Heeney and I. McCulloch, *J. Am. Chem. Soc.*, 2011, **133**, 3272; (b) S. Y. Qu and H. Tian, *Chem. Commun.*, 2012, **48**, 3039; (c) L. T. Dou, J. B. You, J. Yang, C. C. Chen, Y. J. He, S. Murase, T. Moriarty, K. Emery, G. Li and Y. Yang, *Nat. Photonics*, 2012, **6**, 180; (d) Y. N. Li, P. Sonar, L. Murphy and W. Hong, *Energy Environ. Sci.*, 2013, **6**, 1684.

6   (a) J. Lee, A. R. Han, H. Yu, T. J. Shin, C. Yang and J. H. Oh, *J. Am. Chem. Soc.*, 2013, **135**, 9540; (b) I. Kang, H. J. Yun, D. S. Chung, S. K. Kwon and Y. H. Kim, *J. Am. Chem. Soc.*, 2013, **135**, 14896; (c) I. Kang, T. K. An, J. A. Hong, H. J. Yun, R. Kim, D. S. Chung, C. E. Park, Y. H. Kim and S. K. Kwon, *Adv. Mater.*, 2013, **25**, 524.

7   (a) Y. Sun, G. C. Welch, W. L. Leong, C. J. Takacs, G. C. Bazan and A. J. Heeger, *Nat. Mater.*, 2012, **11**, 44; (b) A. K. K. Kyaw, D. H. Wang, V. Gupta, J. Zhang, S. Chand, G. C. Bazan and A. J. Heeger, *Adv. Mater.*, 2013, **25**, 2397; (c) D. Ye, X. Li, L. Yan, W. Zhang, X. Hu, Y. Liang, J. Fang, W. Y. Wong and X. Wang, *J. Mater. Chem. A*, 2013, **1**, 7622; (d) B. Walker, A. B. Tamayo, X. D. Dang, P. Zalar, J. H. Seo, A. Garcia, M. Tantiwiwat and T. Q. Nguyen, *Adv. Funct. Mater.*, 2009, **19**, 3063; (e) Y. Liu, X. Wan, F. Wang, J. Zhou, G. Long, J. Tian, J. You, Y. Yang and Y. Chen, *Adv. Energy Mater.*, 2011, **1**, 771.

8   A. B. Tamayo, B. Walker and T. Q. Nguyen, *J. Phys. Chem. C*, 2008, **112**, 11545.

9   (a) J. E. Coughlin, Z. B. Henson, G. C. Welch and G. C. Bazan, *Acc. Chem. Res.*, 2014, **47**, 257; (b) L. Dou, J. You, Z. Hong, Z.

Xu, G. Li, R. A. Street and Y. Yang, *Adv. Mater.*, 2013, **25**, 6642; (c) Y. Li, *Acc. Chem. Res.*, 2012, **45**, 723; (d) S. D. Dimitrov and J. R. Durrant, *Chem. Mater.*, 2014, **26**, 616.

10 Y. J. Kim, J. Y. Back, S-O. Kim, C-W. Jeon, C. E. Park and Y-H. Kim, *Chem. Asian J*. 2014, **9**, 2505.

11 Q-C. Yu, W-F. Fu, J-H. Wan, X-F. Wu, M-M. Shi and H-Z. Chen, *ACS Appl. Mater*. *Interfaces*, 2014, **6**, 5798.

12 Y. Ren, A. M. Hiszpanski, L. Whittaker-Brooks and Y-L Loo, *ACS Appl. Mater. Interfaces*, 2014, **6**, 14533.

13 (a) J. Liu, B. Walker, A. Tamayo, Y. Zhang and T.-Q. Nguyen*, Adv. Funct. Mater.,* 2013*,* **23**, 47; (b) S.-Y. Liu, M.-M. Shi, J-C. Huang, Z.-N. Jin, X.-L. Hu, J.-Y. Pan, H.-Y. Li, A. K.-Y. Jen and H.-Z. Chen, *J. Mater. Chem. A*, 2013, **1**, 2795; (c) V. S. Gevaerts, E. M. Herzig, M. Kirkus, K. H. Hendriks, M. M. Wienk, J. Perlich, P. Muller-Buschbaum and R. A. J. Janssen, *Chem. Mater.*, 2014, **26**, 916.

14 G. Zhang, H. Li, S. Bi, L. Song, Y. Lu, L. Zhang, J. Yu and L. Wang, *Analyst*, 2013, **138**, 6163.

15 H. Liu, H. Jia, L. Wang, Y. Wu, C. Zhan, H. Fu and J. Yao, *Phys. Chem. Chem. Phys*., 2012, **14**, 14262.

16 (a) M. R. Silva-Junior, M. Schreiber, S. P. A. Sauer and W. Thiel, *J. Chem. Phys.*, 2008, **129**, 104103; (b) M. J. G. Peach, P. Benfield, T. Helgaker and D. J. Tozer, *J. Chem. Phys*. 2008, **128**, 044118.

17   M. C. Hwang, J-W. Jang, T. K. An, C. E. Park, Y-H. Kim and S-K. Kwon, *Macromolecules* 2012, **45**, 4520.

18 A. Kahn, N. Koch and W. Gao, *J. Polym. Sci. B*, 2003, **41** 2529.

19 M. Abbas, A. Pivrikas, E. Arici, N. Tekin, M. Ullah, H. Sitter and N. S. Sariciftci, *J. Phys. D: Appl. Phys*., 2013, **46**, 495105.

20 (a) S. S. Dharmapurikar, A. Arulkashmir, C. Das, P. Muddellu, and K. Krishnamoorthy, *ACS Appl. Mater. Interfaces*, 2013, **5**, 7086; (b) A. Arulkashmir, R. Y. Mahale, S. S. Dharmapurikar, M. K. Jangid and K. Krishnamoorthy, *Polym. Chem.*, 2012, **3**, 1641.

21 Y. Zhang, J. Liu and T.-Q. Nguyen, *ACS Appl. Mater. Interfaces,* 2013, **5**, 2347.

Graphical Abstract

A detailed study on the thermal, photo-physical, electrochemical properties and OFET applications of D-π-A-π-D structured unsymmetrical diketopyrrolopyrrole materials

D. Bharath,[a] S. Chithiravel,[b] M. Sasikumar,[a] Narendra Reddy Chereddy,[a,]* S. Balaih,[c] K. Bhanuprakash,[c,]* K. Krishnamoorthy[b,]* and V. Jayathirtha Rao[a,d]*

[a]*Crop Protection Chemicals Division, [c]Inorganic & Physical Chemistry Division, [d]AcSIR, CSIR-Indian Institute of Chemical Technology, Hyderabad-500 007, India*

[b]*Polymers and Advanced Materials Laboratory, CSIR-National Chemical Laboratory, Pune-411008, India.*

Corresponding author Tel.: +91 40 27193933; +91 40 27193174
E-Mail: **chereddynarendra@gmail.com; jrao@iict.res.in; k.krishnamoorthy@ncl.res.in**
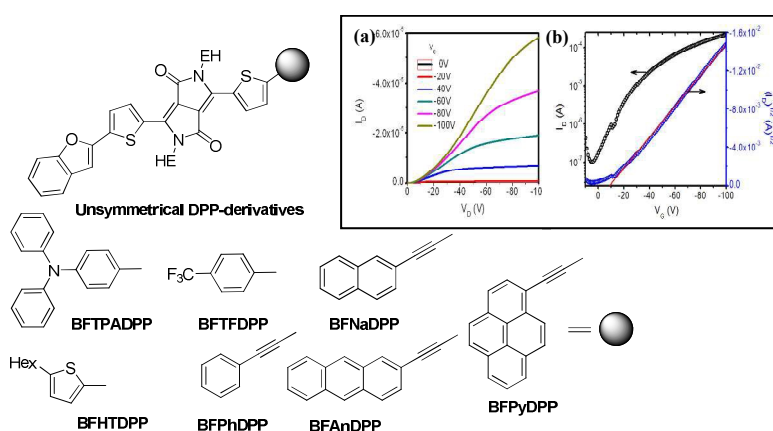
Seven unsymmetrical DPP-derivatives with D-π-A-π-D architecture have been synthesized and the effect of the electron donating ability and extent of electronic conjugation of the end capping units on their thermal, photo-physical, electrochemical and charge carrier transporting properties is explored.